

1 **Capture of *Vibrio cholerae* by charged polymers inhibits pathogenicity by**
2 **inducing a sessile lifestyle**

3
4 Nicolas Perez-Soto^{1,2}, Lauren Moule^{1,2}, Daniel N. Crisan^{2,3}, Ignacio Insua^{2,3}, Leanne M. Taylor-
5 Smith^{1,2}, Kerstin Voelz^{1,2}, Francisco Fernandez-Trillo^{2,3,*}, Anne Marie Krachler^{1,2,*}

6
7 ¹ School of Biosciences, ² Institute of Microbiology and Infection, and ³ School of Chemistry,
8 University of Birmingham, Edgbaston, B15 2TT Birmingham, UK

9
10 *Correspondence to: Anne Marie Krachler (a.krachler@bham.ac.uk) and Francisco Fernandez-
11 Trillo (f.fernandez-trillo@bham.ac.uk)

12

13

14 **ABSTRACT**

15 *Vibrio cholerae*, the causative agent of cholera, is an abundant environmental bacterium that can
16 efficiently colonize the intestinal tract and trigger severe diarrheal illness. Motility, and the
17 production of colonization factors and cholera toxin, are fundamental for the establishment of
18 disease. In the aquatic environment, *V. cholerae* persists by forming avirulent biofilms on
19 zooplankton, phytoplankton and chitin debris. Here, we describe the formation of artificial,
20 biofilm-like communities, driven by exposure of planktonic bacteria to synthetic polymers. This
21 recruitment is extremely rapid and charge-driven, and leads to the formation of initial “seed
22 clusters” which then recruit additional bacteria to extend in size. Bacteria that become entrapped
23 in these “forced communities” undergo transcriptional changes in motility and virulence genes,
24 and phenotypically mimic features of environmental biofilm communities by forming a matrix
25 that contains polysaccharide and extracellular DNA. As a result of this lifestyle transition,
26 pathogenicity and *in vivo* host colonization decrease. These findings highlight the potential of
27 synthetic polymers to disarm pathogens by modulating their lifestyle, without creating selective
28 pressure favoring the emergence of antimicrobial resistant strains.

29

30

31 **SIGNIFICANCE**

32 *Vibrio cholerae* is an important human pathogen and causes watery diarrhea after consumption of
33 contaminated water. Its reservoir are aquatic environments, where it persists in an avirulent
34 biofilm state. Upon ingestion, it escapes biofilms and expresses virulence factors, leading to
35 colonization and pathogenicity within the human host. Here, we show that capture by charged
36 polymers rapidly immobilizes *V. cholerae* and artificially forces it into a sessile state. This
37 mimics environmental cues for biofilm formation and leads to repression of virulence factors
38 through loss of motility. This work highlights a novel artificial lifestyle and an efficient way to
39 neutralize virulent *V. cholerae* and block disease and transmission.

40 INTRODUCTION

41 *Vibrio cholerae* is a Gram-negative bacterium responsible for several million incidences of
42 enteric disease and up to 142,000 deaths every year (1). Many of these cases are attributable to
43 the *V. cholerae* El Tor biotype, which is the cause of an ongoing global epidemic, the 7th to
44 sweep our planet in recorded history. A natural inhabitant of aquatic environments, El Tor's
45 success has been attributed to genetic systems for quorum sensing, chitin breakdown and
46 virulence. Within the human host, the bacterium initiates a virulence programme including the
47 induction of colonization factors and toxins. The two major virulence factors expressed by El Tor
48 strains are cholera toxin and the toxin-coregulated pilus (TCP). Cholera toxin is an ADP-
49 ribosyltransferase of the AB₅ family, which leads to the profuse watery diarrhea and electrolyte
50 loss characteristic of the disease. Its subunits are encoded by *ctxA* and *ctxB* which are organized
51 in an operon(2). TCP, a type IV pilus, is required for formation of bacterial microcolonies in the
52 small intestine and leads to a local enhancement in toxin concentration at the site of infection.
53 The major pilus subunit is encoded by *tcpA*(3, 4). In aquatic environments, *V. cholerae* persists
54 by forming biofilms on the surfaces of phytoplankton, zooplankton and chitin debris (5, 6).
55 Biofilms, which are composed of a matrix of exopolysaccharide and extracellular DNA
56 surrounding the bacteria, offer a protective environment against aquatic predators as well as the
57 host environment. Thus, biofilm formation is an important contributing factor to human disease
58 (7, 8). Efficient colonization of the host intestine, however, requires disassembly of biofilms, and
59 a switch to active motility allowing the bacterium to search out and attach to the host epithelium
60 (8, 9). Indeed, escape from the biofilm is a prerequisite for induction of the virulence programme
61 (8) and failure to escape from the biofilm state results in decreased host colonization fitness *in*
62 *vivo* (10). Clearly, the ability to switch between motile and sessile lifestyles, along with the
63 carefully controlled induction of virulence factors, is central to the establishment of disease and
64 the emergence of Cholera epidemics (11).

65 Although efforts to develop a widely effective vaccine against *V. cholerae* are ongoing, the
66 efficacy of existing vaccines is low. Attenuated *V. cholerae*, for example, elicits protective
67 immunity in as few as 16% of patients in developing countries (12). In addition, current vaccines
68 offer protection for only two years, a time period shorter than many epidemics. Currently, and in
69 the absence of a vaccination program, the best way to prevent such outbreaks is by water

70 treatment and provision of sanitation infrastructure. As such, low-tech measures to facilitate
71 decontamination of drinking water, such as simple means of filtration, are desirable and can have
72 a dramatic impact on disease incidence (13). Moreover, there is a lack of understanding of how *V.*
73 *cholerae* responds to these strategies, and how this pathogen regulates virulence and motility
74 upon immobilization onto a filtration device. To this end, we demonstrate here that linear,
75 cationic polymers can rapidly capture *V. cholerae* from aqueous environments and, upon
76 sequestration into these artificially precipitated communities, induce an avirulent phenotype in *V.*
77 *cholerae* that mimics environmental biofilm formation. Overall, the polymers force *V. cholerae*
78 into an artificial sessile lifestyle, which inhibits virulence factor production, colonization and
79 dissemination.

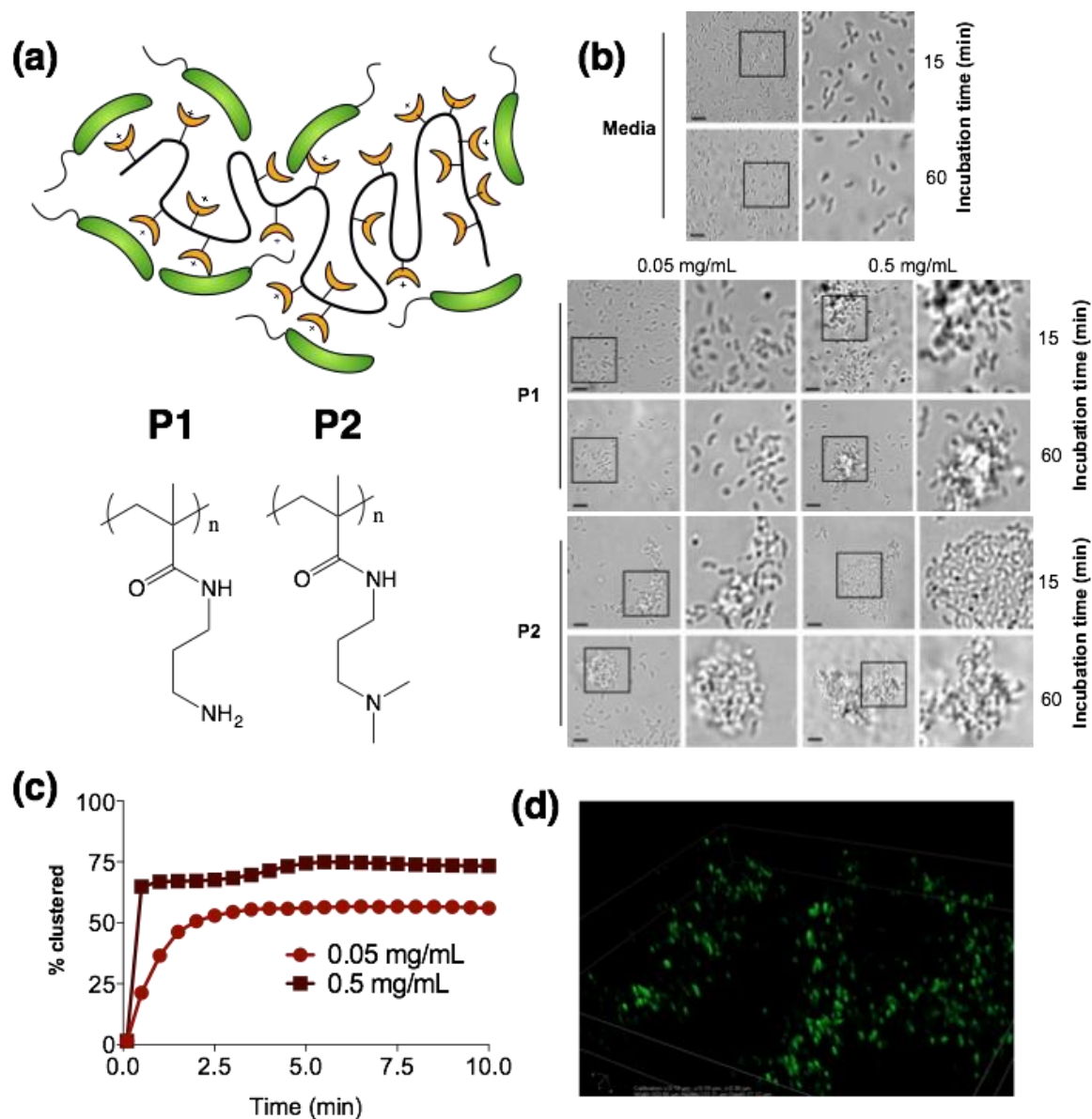
80

81 RESULTS

82 Cationic polymers rapidly form three-dimensional clusters upon contact with *V. cholerae*.

83 Many polycationic polymers have been designed to maximize their antimicrobial effects (14-16)
84 and previously published work demonstrated a trade-off between the charge and hydrophobicity
85 in cationic polymers and their ability to cluster bacteria, and/or affect bacterial viability within
86 clusters (17-19). Based on our previous work with closely related species *Vibrio harveyi* (17, 18),
87 we decided to investigate the potential of (poly(*N*-(3-aminopropyl)methacrylamide), pAPMAm –
88 P1 and (poly(*N*-[3-(dimethylamino)propyl]methacrylamide), pDMAPMAm - P2, to remove *V.*
89 *cholerae* from aqueous environments (**Figure 1a**). These polymers are both cationic under
90 neutral aqueous conditions and were synthesized via free radical polymerization with high purity
91 (**Figure S1** and **Figure S2**). Upon contact with *V. cholerae*, both polymers rapidly formed
92 clusters *in situ* in a concentration dependent manner (**Figure 1b**), and cluster formation reached
93 equilibrium within minutes (**Figure 1c**). Cluster formation proceeded via initial nucleation of
94 small layers or sheets of bacteria, which increased in size both by lateral interaction with
95 additional bacteria, as well as stacking of bacteria on existing sheets to form clusters over the first
96 15 minutes, and then remained stable over the duration of the experiment (**Figure 1b,d**). No
97 significant differences were observed between both polymers, suggesting that clustering was
98 mainly dominated by electrostatic interactions between the positively charged polymers and the
99 negatively charged bacteria. Bacterial clusters were stable for at least 24 hours and had a well-

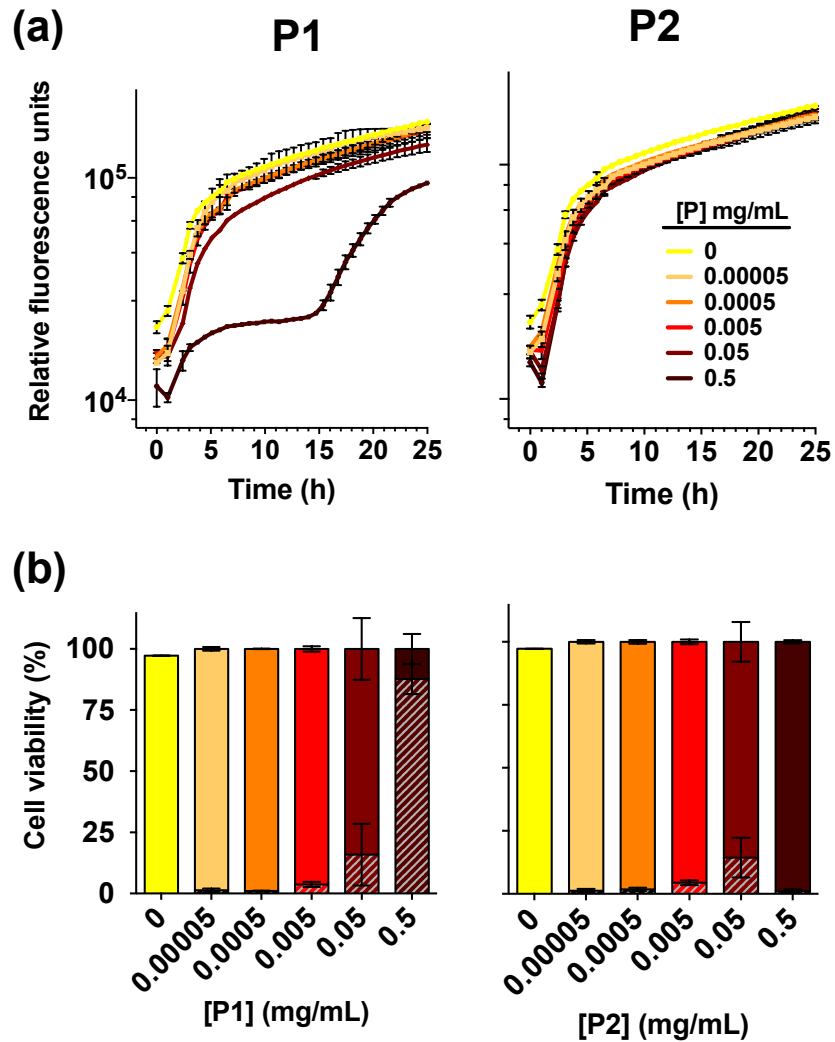
100 defined three-dimensional structure (**Figure 1d** and **Figure S3**). Both polymers induced bacterial
 101 clustering with high efficiency, and the endpoints were practically indistinguishable in terms of
 102 numbers of particles and cluster size (**Figure 1b**).



103
 104 **Figure 1 | Cationic polymers rapidly form three-dimensional clusters upon contact with *Vibrio cholerae*.** (a)
 105 Bacteria are clustered via electrostatic interactions between polymers containing positively charged sidechains
 106 (yellow) and *V. cholerae* (green). Chemical structures of polymers P1 and P2 are shown. (b) Clusters formed after
 107 incubation of *V. cholerae* with 0.05 or 0.5 mg/mL of P1 or P2 for 15 or 60 min were visualized by microscopy using
 108 a DIC filter (c) Concentration-dependent kinetic analysis of particle size distribution for P1-induced bacterial
 109 clustering. Particle size distribution was analyzed using a Mastersizer. Clusters are defined as particles of a mean
 110 diameter larger than that of individual bacteria (2 μ m). (d) Clusters formed after incubation of GFP-*V. cholerae* with

111 0.5 mg/mL of P1 for 15 minutes were visualized by spinning disc fluorescence microscopy. Images are
112 representative of at least three independent experiments.

113 **Effect of polymer-induced clustering on bacterial growth and membrane integrity.** The
114 effect of cationic polymers on bacterial viability varies significantly with charge, hydrophobicity,
115 polymer concentration and the bacterial species tested (17, 18). Thus, we explored if and how
116 clustering of *V. cholerae* affects bacterial proliferation and viability under physiological
117 conditions. Bacterial proliferation during co-incubation of GFP expressing *V. cholerae* with
118 different concentrations of polymers was measured, monitoring GFP fluorescence over 25 hours
119 (**Figure 2a**). Bacterial proliferation was generally unaffected, except at very high polymer
120 concentrations (0.5 mg/ml of P1, **Figure 2a**). However, it was unclear from these experiments
121 whether the slower increase in fluorescence was due to inhibition of bacterial growth, as is
122 observed within subsets of cells within bacterial biofilms (11), or due to cellular damage
123 commonly observed with highly charged cationic polymers (19). Flow cytometry of bacterial
124 samples exposed to polymers and LIVE/DEAD® cell viability stains allowed us to determine
125 bacterial viability via measuring membrane integrity of *V. cholerae* sequestered in clusters at the
126 experimental endpoint (**Figure 2b**). Viability and membrane integrity were largely unaffected by
127 clustering even following overnight incubation, except at very high polymer concentrations (0.5
128 mg/ml P1, **Figure 2b**). We also investigated the effect of both polymers on host cells, in this case
129 cultured Caco-2 intestinal epithelial cells, using lactate dehydrogenase release (LDH) assays to
130 probe cellular membrane integrity (**Figure S4**). P1 and P2 both compromised membrane integrity
131 of epithelial cells at $5 \cdot 10^{-3}$ and $5 \cdot 10^{-4}$ mg/mL or above, respectively, compared to untreated
132 control cells. Thus, for functional experiments, we focused on investigating the effects of the
133 highest effective, non-toxic concentration of both polymers.



134

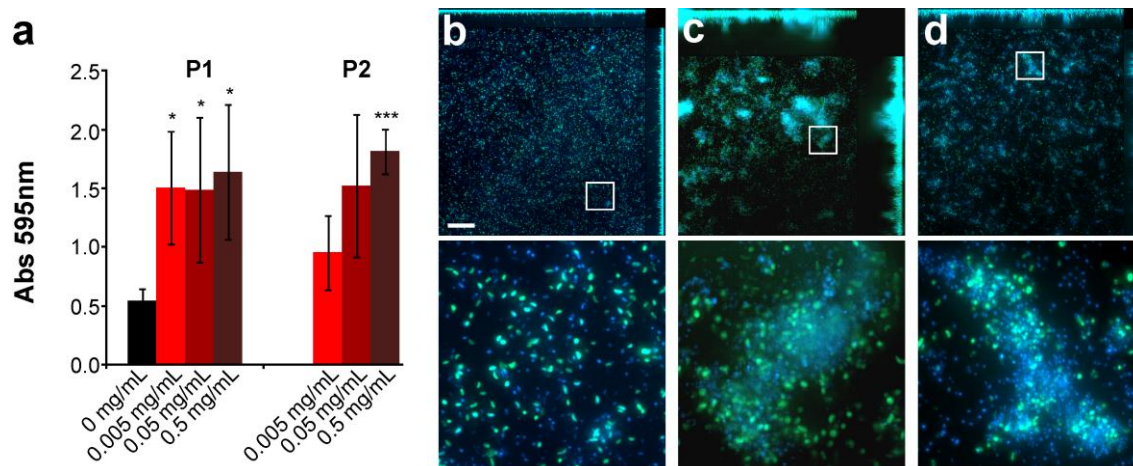
135 **Figure 2 | Effect of polymer-induced clustering on bacterial growth and viability.** (a) GFP-*V. cholerae* were
 136 adjusted to an initial OD₆₀₀ of 0.02, added to polymers to give final concentrations as indicated in the legend, and
 137 grown under shaking at 37 °C for 24 hrs, with GFP fluorescence measured every 30 min. Results are means ± s.e.m.
 138 of three independent experiments. (b) *V. cholerae* were adjusted to an initial OD₆₀₀ of 1, added to polymers to give
 139 final concentrations as indicated, and incubated overnight. Samples were stained for membrane integrity using a
 140 LIVE/DEAD™ cell viability kit and analyzed by flow cytometry. Experimental samples were gated using untreated
 141 (viability 100%) and 2-propanol treated (viability 0%) samples as controls. % bacteria gates as live (filled columns)
 142 and dead (hatched columns), respectively, are shown, with results representing means ± s.e.m. from three
 143 independent experiments.

144

145 **Sequestration of *V. cholerae* into polymer clusters induces a biofilm-like state and**
 146 **suppresses bacterial virulence at the transcriptional level.** The switch to a sessile lifestyle and
 147 biofilm formation in *V. cholerae* is initiated by surface sensing and downregulation of bacterial

148 motility (11, 20). Since we observed during imaging experiments that bacterial clustering
149 abrogated bacterial motility, we investigated whether polymer-induced clustering would also
150 affect *in vitro* biofilm formation. Polymer-induced clustering lead to a significant induction of
151 biofilm formation in *V. cholerae*, as measured using crystal violet assays and imaging of GFP-*V.*
152 *cholerae* (**Figure 3a**). Polymer-induced biofilms also released higher levels of extracellular DNA
153 into the biofilm, compared to untreated *V. cholerae* (**Figure 3b-d**).

154



155

156 **Figure 3 | Polymer-induced clustering leads to increased *V. cholerae* biofilm formation.** Biofilm formation of *V.*
157 *cholerae* after overnight incubation in the absence or presence of polymers **P1** or **P2** at concentrations as indicated,
158 was quantified using crystal violet plate assays (**a**). Analysis of variance (ANOVA), followed by Tukey's post hoc
159 test, was used to test for significance. Statistical significance was defined as $p < 0.05$ (*), $p < 0.01$ (**) or $p < 0.001$
160 (***). Biofilms of GFP-*V. cholerae* were imaged following 20 hours of growth in glass-bottom plates at 37 °C, in
161 DMEM only (**b**), or DMEM containing 0.05 mg/mL P1 (**c**) or 0.5 mg/mL P2 (**d**). Samples were fixed and DNA was
162 stained with Hoechst (blue). Scale bar, 50 μm. Area within the square has been expanded (bottom row) for clarity.

163

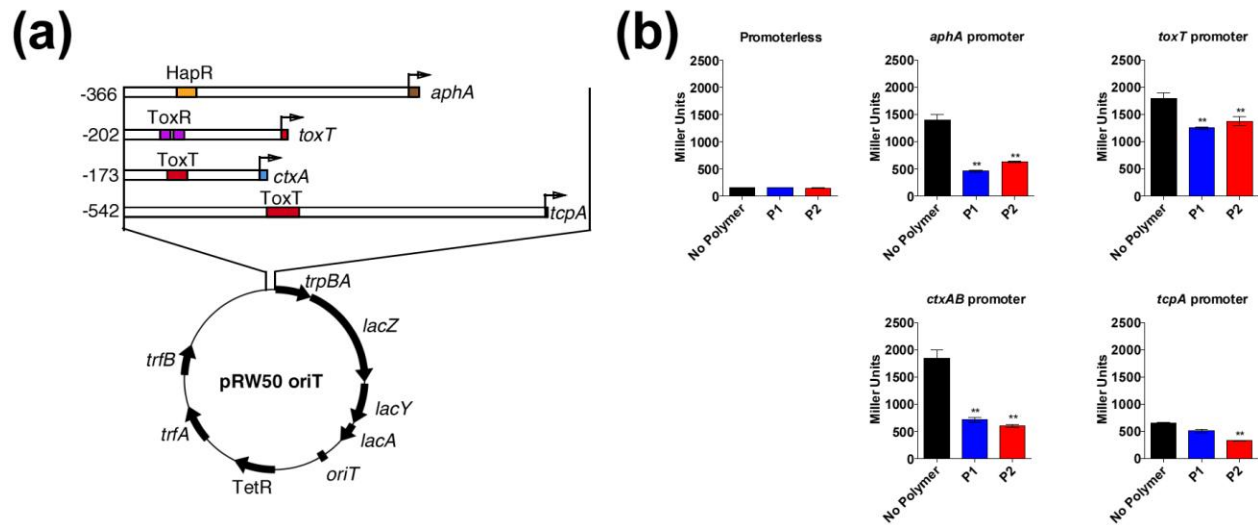
164 Since sequestration into polymer clusters promotes a sessile state, we investigated what impact
165 this environmental signal would have on virulence regulation. For this purpose, we created a
166 series of transcriptional reporter strains, by introducing, via conjugation, a variant of the pRW50
167 plasmid containing *oriT* into *V. cholerae* (**Figure 4a**). Thus, we could follow the induction of *V.*
168 *cholerae* promoters during growth in medium mimicking inducing conditions within the host
169 environment (DMEM, 37 °C), using β -galactosidase assays. AphA is a master regulator of

170 virulence that is required for the activation of *tcpP*. TcpP, in turn, activates *toxT*, which activates
171 downstream virulence genes, including those responsible for the production of cholera toxin and
172 the toxin-coregulated pilus (TCP). In the absence of polymer, the *aphA* promoter was strongly
173 induced (~9-fold compared to vector control) in mid-log phase cells (**Figure 4b**). Sequestration
174 of *V. cholerae* into clusters significantly repressed the *aphA* promoter activity (approx. 70% and
175 55% suppression with **P1** and **P2**, respectively). The *toxT* promoter was also strongly induced
176 (~12-fold over vector control) in the absence of polymer but significantly repressed in bacterial
177 clusters (~30% and 20% inhibition by **P1** and **P2**, respectively). Similarly, the promoters of the
178 two key virulence factors, *ctxAB* and *tcpA*, were strongly induced under conditions mimicking the
179 host environment (12-fold and 4-fold induction over vector control, respectively) with both **P1**
180 and **P2** suppressing *ctxAB* transcription by approximately 60% and 70%, respectively. The effect
181 on *tcpA* was less pronounced, with **P1** showing only mild suppression, and **P2** suppressing
182 transcription by ~50% (**Figure 4b**). We also investigated the effect of physical immobilization
183 within artificial clusters on transcriptional regulation of genes encoding for components of the
184 flagellar systems (*flaE* and *flaA*, respectively). Both of these were comparatively weak promoters
185 (~2 to 2.5-fold induction compared to vector control). Interestingly, both *flaE* and *flaA* were
186 downregulated by P1 mediated clustering, while P2, which is more hydrophobic than **P1**, had no
187 effect on *flaA* or *flaE* transcription levels (**Figure S5**).

188

189

190



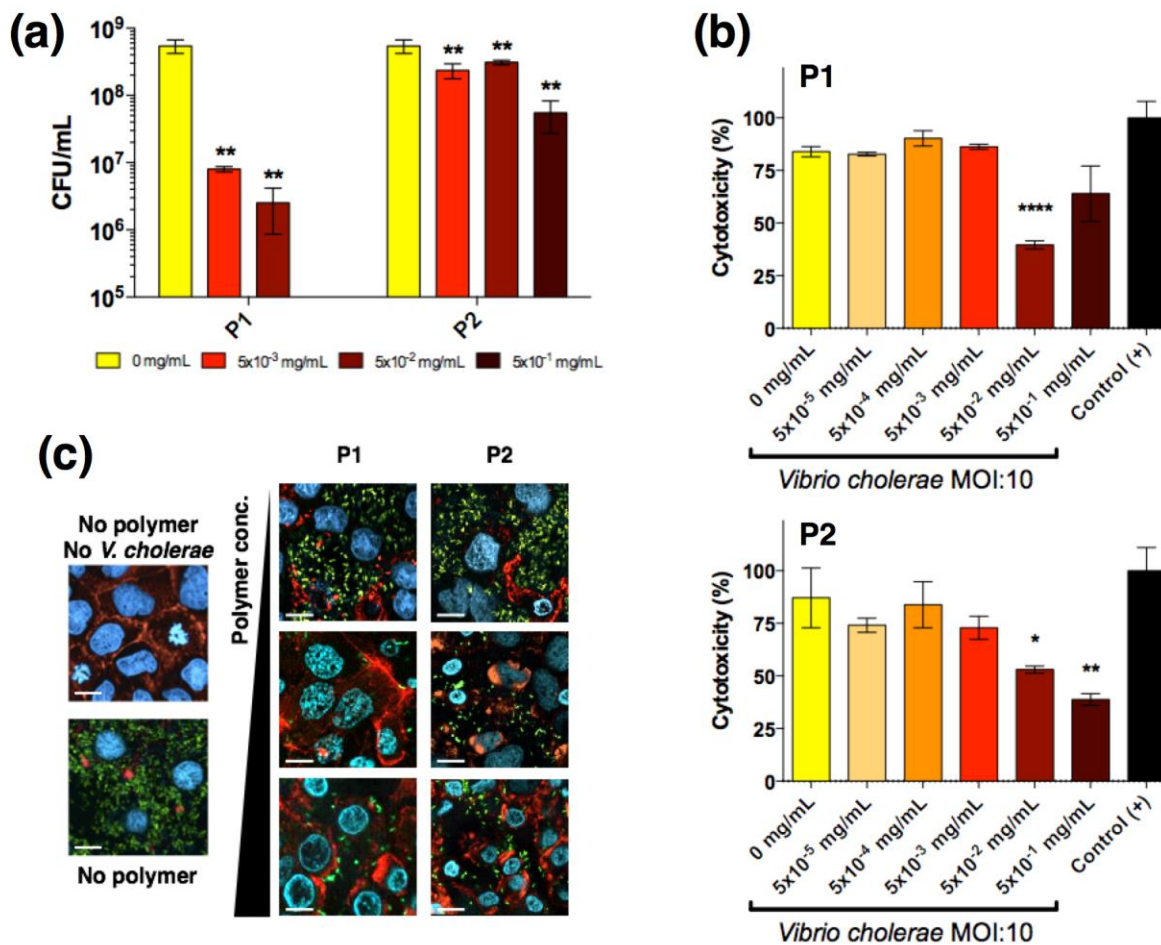
191

192 **Figure 4 | Sequestration of *V. cholerae* into polymer clusters suppresses bacterial virulence at the**
 193 **transcriptional level.** (a) Schematic depiction of the reporter plasmid (pRW50-*oriT*) and promoter regions of *aphA*,
 194 *toxT*, *ctxA* and *tcpA* cloned as transcriptional fusions to *lacZ* in pRW50-*oriT*. Numbering refers to base number
 195 relative to the transcriptional start site. (b) Promoter activities of *aphA*, *toxT*, *ctxA* and *tcpA* promoter-*lacZ* fusions
 196 were measured following 7 hours of growth in the absence (black) or presence of 0.05 mg/mL P1 (blue) or 0.5
 197 mg/mL P2 (red).

198

199 **Polymer sequestration of bacteria abolishes *V. cholerae* infection *in vitro* and intestinal**
 200 **colonization *in vivo*.** Since polymer-induced clustering repressed the induction of key virulence
 201 factors, we asked what impact clustering would have on *V. cholerae* infection. Initially, we tested
 202 the effect of clustering on colonization and toxicity towards cultured intestinal epithelial cells.
 203 Sequestration of *V. cholerae* by polymers led to a significant reduction in bacterial attachment to
 204 host cells, as determined both by dilution plating/CFU counts and imaging of infected cells
 205 (**Figure 5a-c**). Imaging of Caco-2 cells infected with either planktonic or clustered *V. cholerae*
 206 also revealed a decrease in *V. cholerae* mediated toxicity as a result of bacterial clustering. Host
 207 cells infected with clustered bacteria showed less cell death and more intact cell-cell junctions
 208 than cells infected with planktonic bacteria (**Figure 5c**). This protective effect of the polymers
 209 was also observed when cytotoxicity was measured by LDH release assays, following infection
 210 with planktonic or clustered *V. cholerae* (**Figure 5b**).

211



212

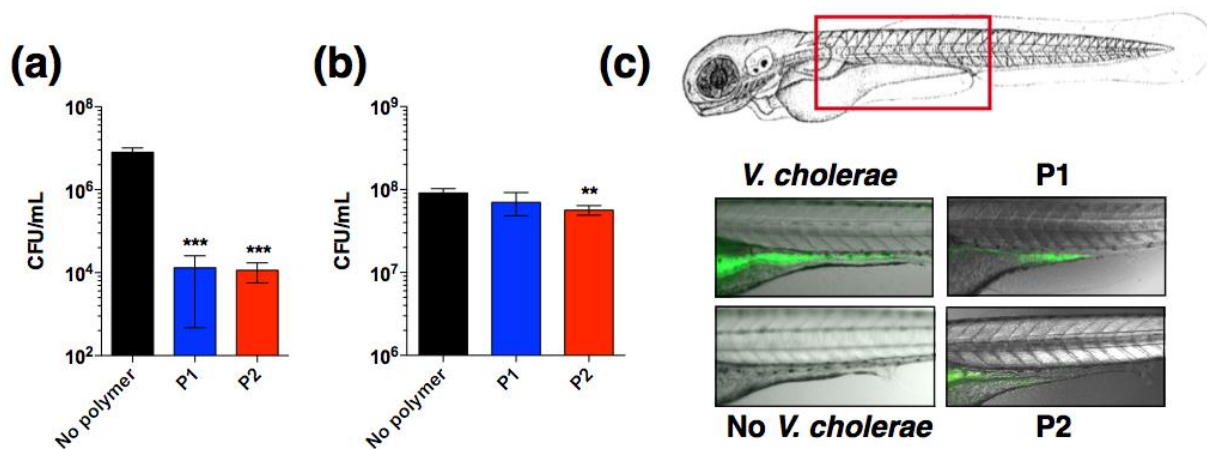
213 **Figure 5 | Polymer sequestration of bacteria abolishes *V. cholerae* infection of cultured epithelial cells.** *V.*
 214 *cholerae* were adjusted to an MOI of 10, and incubated in the absence or presence of polymers for 1 hr prior to
 215 infection of cultured Caco-2 intestinal epithelial cells for 7 hrs. Following the infection, (a) bacteria attached to
 216 Caco-2 cells were quantified by dilution plating, following washing and lysis of Caco-2 cells. (b) Cytotoxic effect on
 217 host cells was quantified by measuring the amount of lactate dehydrogenase (LDH) released into the culture medium.
 218 Results were normalized to untreated Caco-2 cells (0%) and cells lysed with Triton X-100 (100%). Results in a and b
 219 are means \pm s.e.m. of three independent experiments. Analysis of variance (ANOVA), followed by Tukey's post hoc
 220 test, was used to test for significance. Statistical significance was defined as $p < 0.05$ (*), $p < 0.01$ (**) or $p < 0.0001$
 221 (****). (c) Following infection, *V. cholerae* (green), DNA (blue), and F-actin (red) were visualized by fluorescence
 222 microscopy. Scale bar, 10 μ m.

223

224 Finally, we tested whether non-bactericidal concentrations of polymers would protect against
 225 intestinal colonization by *V. cholerae* *in vivo*. Previously, zebrafish (*Danio rerio*) have been
 226 established as an aquatic host which can be colonized and infected by *V. cholerae* in a

227 concentration dependent manner, and infection eventually leads to mortality (21, 22). We tested
228 if bacterial clustering would affect subsequent colonization of zebrafish larvae by *V. cholerae*
229 following a 6 hour exposure. Zebrafish larvae exposed to either 10^7 or 10^8 CFU/mL of planktonic
230 or polymer-clustered GFP-expressing *V. cholerae* were first imaged and then sacrificed, and
231 intestinal *V. cholerae* were extracted from the tissue and enumerated by dilution plating on
232 selective TCBS agar (**Figure 6a-b**). Images of infected fish showed that GFP-expressing *V.*
233 *cholerae* had specifically colonized the gastrointestinal tract, with the majority of bacteria
234 attached to the mid-intestine (**Figure 6c**). The bacterial burden was visibly lower in fish infected
235 with clustered bacteria, compared to fish infected with planktonic bacteria. Bacterial
236 sequestration was more efficient in blocking colonization at an infectious dose of 10^7 (**Figure 6a**)
237 where bacterial burden was reduced more than 100-fold. At a dose of 10^8 *V. cholerae*,
238 colonization was still significantly inhibited by polymer-induced clustering, albeit the effect was
239 much smaller (**Figure 6b**).

240



241

242 **Figure 6 | Polymer sequestration of bacteria abolishes *V. cholerae* colonization in a zebrafish larval infection**
243 **model.** (a) 10^7 or (b) 10^8 CFU/mL of *V. cholerae* were incubated in the absence or presence of polymer (0.05 mg/mL
244 of **P1** or 0.5 mg/mL of **P2**), as indicated, for 1 hr prior to infection experiments. Zebrafish larvae (n=10 per
245 experimental condition) were transferred into bacterial cluster solutions, and incubated for 6 hrs. Larvae were
246 washed in PBS and homogenized using Triton X-100. Bacterial loads were quantified using dilution plating on
247 selective agar. Analysis of variance (ANOVA), followed by Tukey's post hoc test, was used to test for significance.
248 Statistical significance was defined as $p < 0.01$ (**), $p < 0.001$ (***), or $p < 0.0001$ (****). (c) Imaging of zebrafish
249 infected with GFP-*V. cholerae* exposed to 0.05 mg/mL of P1 or 0.5 mg/mL of P2.

250

251 DISCUSSION

252 The interaction between bacteria and polycationic molecules plays an important role in nature.
253 Many antimicrobial peptides are polycationic, and their interactions with and impact on bacterial
254 physiology is well characterized (23, 24). Polycationic synthetic polymers have been researched
255 as a cheaper and more stable alternative to mimic the effect of naturally occurring AMPs, and
256 their design and use in previous studies is often targeted at maximizing their antimicrobial effects
257 (25-27). Recent work has however highlighted the potential of such materials to bind bacteria
258 with the aim to manipulate bacterial behaviors, such as quorum sensing, without impacting
259 bacterial viability (17, 18). In the face of increasing problems with the emergence of antibiotic
260 resistant bacterial strains in clinical settings, such strategies, which would potentially provide less
261 selective pressure on the emergence of drug-resistance, become more and more relevant (28). For
262 *V. cholerae*, alternative approaches targeting virulence, rather than bacterial viability, have been
263 the topic of previous research for some time, underpinning the need for novel ways to prevent
264 and treat infections with this globally important human pathogen (29, 30). Anti-adhesion
265 therapies are often proposed as attractive anti-virulence strategies, that compromise the ability of
266 the pathogen to colonise the host and thus establish an infection (31, 32). Similarly, removal of
267 the pathogen through sequestration is often proposed as a cost-effective approach to
268 decontaminate water sources. However, little is known about *V. cholerae* response to these
269 artificial environments and how binding to these materials may affect regulation of virulence in
270 these pathogens.

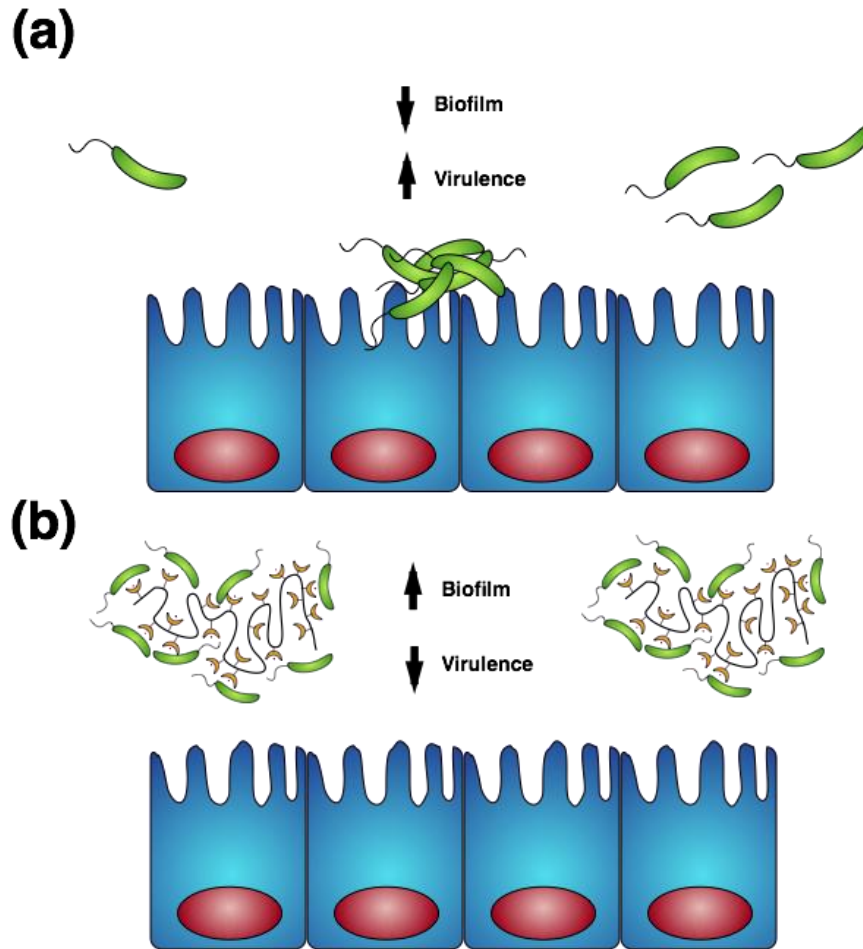
271 With this in mind, we set out to synthesize a set of two polymers with different cationic groups,
272 but identical backbones, to evaluate their impact on bacterial clustering and behavior in *V.*
273 *cholerae*. Based on our previous research with *V. harveyi* (17, 18), pAPMAM – P1 and
274 pDMAPMAM - P2, were investigated. We anticipated that P1 would present higher toxicity
275 towards both bacteria and host cells (**Figure 2** and **Figure S4**) (14-16). We found that both
276 polymers were able to induce clustering of *V. cholerae* irrespective of their cationic nature, and
277 the clusters quickly became big enough to precipitate out of solution (**Figure 1**). Both polymers
278 had little impact on bacterial growth, viability and membrane permeability, in particular at
279 concentrations below 0.05 mg/mL (**Figure 2**). Overall, P1 has a bigger effect on bacterial growth
280 and viability than P2, (**Figure 2**), but even P1 showed bactericidal activity only at the highest

281 concentration tested (0.5 mg/ml). Similarly, charge and buffering impacted on eukaryotic
282 membrane integrity, with both P1 and P2 able to disrupt host cell membranes at high
283 concentrations (**Figure S4**). For both materials, this cytotoxicity would result in a narrow
284 therapeutic window, and thus future applications of polymers inducing bacterial clustering by
285 electrostatic interactions alone would likely lean more towards an *ex vivo* preventative
286 application, for example as part of a low-tech water decontamination/filtration strategy. Although
287 this is in itself a promising approach, our future efforts will also focus on the synthesis of
288 materials with decreased toxicities that exhibit high affinity towards the bacteria by other means
289 (e.g. incorporation of natural ligands for *V. cholerae* such as N-acetyl-glucosamine into the
290 polymer). This approach may open up new avenues to extend future applications of such
291 materials towards a prophylactic or therapeutic use in patients.

292 Infectious *V. cholerae* are often taken up as small biofilms, from which bacteria escape to
293 colonize the epithelium. Once bound, bacteria initiate microcolony formation, before eventually
294 exiting the host's GI tract, often following re-organization into biofilms (33, 34), to cause
295 environmental dispersal and onward-transmission. The ability to transition between motile and
296 sessile states is thus key to *V. cholerae*'s virulence regulation upon entering the human host and
297 initialization of its colonization programme. Active bacterial motility and induction of virulence
298 factors are both crucially required for *V. cholerae* pathogenesis. In natural environments, the
299 transition of *V. cholerae* to a sessile lifestyle and inhibition of motility is accomplished both by
300 transcriptional repression of flagellar genes, as well as induction of extracellular polysaccharide
301 production, both of which are mediated by c-di-GMP (35). The cues triggering these motile to
302 sessile transition in *V. cholerae* are still subject to investigations, but recent work showed that
303 both lowered temperatures as well as type IV pili-mediated surface sensing can feed into c-di-
304 GMP signaling and thus biofilm formation (36, 37). With our polymers bacterial motility is also
305 largely abolished, albeit by physical deposition into polymer-based clusters. Interestingly, while
306 both polymers cause immobilization to a similar extent, P1 but not P2 caused transcriptional
307 repression of flagellar genes (**Figure S5**). This suggests that physicochemical properties of the
308 adhesive surface, rather than the mechanical process of surface sensing alone, also impact the
309 transition to a sessile lifestyle. Interestingly, despite their different effects on gene regulation in
310 response to immobilization, both polymers lead to an increase in bacterial deposition on an
311 abiotic surface upon bacterial clustering, which was accompanied by an increased release in

312 extracellular DNA (**Figure 3b-d**). This increase would suggest that these polycationic polymers
313 may act as an alternative cue to promote a transition toward a sessile, community-based lifestyle
314 for *V. cholerae*. At the same time, clustering of *V. cholerae* lead to a decrease in virulence factors
315 at the transcriptional level (**Figure 4b**). Regulation of virulence genes in *V. cholerae* is a complex
316 process and several pathways converge at this point. Crucially, both high cell density, via quorum
317 sensing, and c-di-GMP dependent signaling can act to repress virulence genes (38, 39). Based on
318 the fact that a “biofilm-like state” is induced by clustering in our system, while quorum sensing
319 leads to HapR-dependent suppression of biofilm formation, we conclude that the transcriptional
320 repression of virulence genes we observe here is triggered by a cue that mimics more closely the
321 transition towards a sessile lifestyle in aquatic environments, rather than high cell density
322 dependent signaling. The net effect of this polymer-induced phenotypical switch towards
323 avirulence is a decrease in colonization and a decrease in cytotoxicity towards cultured cells
324 (**Figure 5**).

325 Finally, we evaluated the potential of these dual-action polymers to inhibit infection in an *in vivo*
326 model. Zebrafish are a suitable natural host model for *V. cholerae* colonization and transmission
327 (21, 22) as their gastrointestinal development and physiology closely mimics that of mammalian
328 organisms (40). Additionally, ease of propagation and live imaging made them a good choice of
329 host for our *in vivo* studies. Due to license restrictions on the experimental duration in the
330 zebrafish infection model, we were unable to characterize the effect of *V. cholerae* on zebrafish
331 survival. However, the observed decrease in initial colonization (**Figure 6**) supports the notion
332 that clustering would be an effective way to “neutralize” *V. cholerae in vivo*. Overall, our results
333 show that the tested materials mainly act to modulate bacterial behavior in a way that positively
334 impacts on the outcome of infection (**Figure 7**).



335

336 **Figure 7 | Dual action polymers abrogate *V. cholerae* infection by physical and transcriptional interference**
337 **with host colonization and virulence.** (a) *V. cholerae* are often ingested as small biofilms, from which they escape
338 to initiate infection of the host intestinal epithelium. Downregulation of biofilm genes and upregulation of virulence
339 genes, such as cholera toxin and toxin-coregulated pilus, are necessary for successful infection. (b) Polycationic
340 polymers form clusters of *V. cholerae*. Clustering abolishes active motility, induces a biofilm-like state, and leads to
341 a downregulation of virulence genes. This dual mode of action inhibits infection of the intestinal epithelium.

342

343 **Conclusions**

344 Here, we have shown that linear polymers that can sequester the human pathogen *V. cholerae*
345 into clusters, downregulate virulence and mitigate colonization and toxicity in relevant *in vitro*
346 and *in vivo* models. Using cationic polymers and a combination of phenotypic and transcriptional
347 assays, we demonstrate that this reduction in virulence is a result of *V. cholerae* switching to a
348 non-pathogenic environmental-like phenotype upon clustering. Our observations suggest that

349 polymeric materials can underpin the development of novel cost-effective strategies to minimize
350 *V. cholerae* pathogenicity without promoting antimicrobial resistance. As such we anticipate that
351 these materials can act as a blueprint for the development of novel cost-effective prophylactic or
352 therapeutic polymers, but to this end, a clear understanding of how these materials trigger
353 phenotypic responses in these pathogens is essential. Our efforts to optimize affinity toward *V.*
354 *cholerae* while minimizing toxicity towards the host will be reported in due course.

355

356 **MATERIALS AND METHODS**

357 Polymers used in this study were poly-*N*-(3-aminopropyl)methacrylamide p(APMAm), P1 and
358 poly-*N*-[3-(dimethylamino)propyl]methacrylamide p(DMAPMAm), P2. Their synthesis and
359 characterization, as well as their use in biological assays, are described in detail in the Supporting
360 Materials and Methods.

361 **ACKNOWLEDGEMENTS**

362 We thank D. Grainger and his group for their advice on the construction of transcriptional
363 reporter plasmids. We thank members of the Krachler and Fernandez-Trillo labs for critical
364 reading and comments on the manuscript. This work was supported by University of Birmingham
365 Fellowships (to A.M.K. and F.F.-T.), Wellcome Trust grant 177ISSFPP (to A.M.K. and F.F.-T),
366 BBSRC grants BB/M021513/1 (to K.V. and A.M.K.) and BB/L007916/1 (to A.M.K.), BBSRC
367 MIBTP studentships (to L.M.) and a CONICYT fellowship (to N.P.-S.).

368 **CONTRIBUTIONS**

369 All authors contributed to the experimental set-up and discussed the results. A.M.K, F.F.-T. and
370 K.V. secure funding. N.P.-S., L.M., I.I. and D.N.C. synthesised and characterised the polymers.
371 N.P.-S., L.M., K.V., A.M.K. performed the biological assays. N.P.-S., K.V., A.M.K. and F.F.-T.
372 analysed the data, and N.P.-S., K.V., A.M.K. and F.F.-T. wrote the manuscript, with all other
373 authors contributing to its final version.

374 **Declaration of competing interests**

375 None to declare.

376 **REFERENCES**

- 377 1. Ali M, *et al.* (2012) The global burden of cholera. *Bulleting of the World Health Organization*.
378 90:209-218A. 10.2471/BLT.11.093427.
- 379 2. Kaper JB, Morris JG, Jr., & Levine MM (1995) Cholera. *Clinical microbiology reviews* 8(1):48-86.
- 380 3. Herrington DA, *et al.* (1988) Toxin, toxin-coregulated pili, and the toxR regulon are essential for
381 *Vibrio cholerae* pathogenesis in humans. *J Exp Med* 168(4):1487-1492.
- 382 4. Thelin KH & Taylor RK (1996) Toxin-coregulated pilus, but not mannose-sensitive hemagglutinin,
383 is required for colonization by *Vibrio cholerae* O1 El Tor biotype and O139 strains. *Infection and*
384 *immunity* 64(7):2853-2856.
- 385 5. Tamplin ML, Gauzens AL, Huq A, Sack DA, & Colwell RR (1990) Attachment of *Vibrio cholerae*
386 serogroup O1 to zooplankton and phytoplankton of Bangladesh waters. *Applied and*
387 *environmental microbiology* 56(6):1977-1980.
- 388 6. Rawlings TK, Ruiz GM, & Colwell RR (2007) Association of *Vibrio cholerae* O1 El Tor and O139
389 Bengal with the Copepods *Acartia tonsa* and *Eurytemora affinis*. *Applied and environmental*
390 *microbiology* 73(24):7926-7933.
- 391 7. Zhu J & Mekalanos JJ (2003) Quorum sensing-dependent biofilms enhance colonization in *Vibrio*
392 *cholerae*. *Developmental cell* 5(4):647-656.
- 393 8. Hay AJ & Zhu J (2015) Host intestinal signal-promoted biofilm dispersal induces *Vibrio cholerae*
394 colonization. *Infection and immunity* 83(1):317-323.
- 395 9. Butler SM & Camilli A (2005) Going against the grain: chemotaxis and infection in *Vibrio*
396 *cholerae*. *Nature reviews. Microbiology* 3(8):611-620.
- 397 10. Seper A, *et al.* (2011) Extracellular nucleases and extracellular DNA play important roles in *Vibrio*
398 *cholerae* biofilm formation. *Molecular microbiology* 82(4):1015-1037.
- 399 11. Teschler JK, *et al.* (2015) Living in the matrix: assembly and control of *Vibrio cholerae* biofilms.
400 *Nature reviews. Microbiology* 13(5):255-268.
- 401 12. Levine MM (2010) Immunogenicity and efficacy of oral vaccines in developing countries: lessons
402 from a live cholera vaccine. *BMC biology* 8:129.
- 403 13. Colwell RR, *et al.* (2003) Reduction of cholera in Bangladeshi villages by simple filtration.
404 *Proceedings of the National Academy of Sciences of the United States of America* 100(3):1051-
405 1055.
- 406 14. Som A, Vemparala S, Ivanov I, & Tew GN (2008) Synthetic mimics of antimicrobial peptides.
407 *Biopolymers* 90(2):83-93.
- 408 15. Scott RW, DeGrado WF, & Tew GN (2008) De novo designed synthetic mimics of antimicrobial
409 peptides. *Current opinion in biotechnology* 19(6):620-627.
- 410 16. Kuroda K & Caputo GA (2013) Antimicrobial polymers as synthetic mimics of host-defense
411 peptides. *Wiley interdisciplinary reviews. Nanomedicine and nanobiotechnology* 5(1):49-66.
- 412 17. Lui LT, *et al.* (2013) Bacteria clustering by polymers induces the expression of quorum-sensing-
413 controlled phenotypes. *Nature chemistry* 5(12):1058-1065.
- 414 18. Xue X, *et al.* (2011) Synthetic polymers for simultaneous bacterial sequestration and quorum
415 sense interference. *Angew Chem Int Ed Engl* 50(42):9852-9856.
- 416 19. Louzao I, Sui C, Winzer K, Fernandez-Trillo F, & Alexander C (2015) Cationic polymer mediated
417 bacterial clustering: Cell-adhesive properties of homo- and copolymers. *European journal of*
418 *pharmaceutics and biopharmaceutics : official journal of Arbeitsgemeinschaft fur*
419 *Pharmazeutische Verfahrenstechnik e.V* 95(Pt A):47-62.
- 420 20. Silva AJ & Benitez JA (2016) *Vibrio cholerae* Biofilms and Cholera Pathogenesis. *PLoS neglected*
421 *tropical diseases* 10(2):e0004330.

- 422 21. Wang H, *et al.* (2012) Catalases promote resistance of oxidative stress in *Vibrio cholerae*. *PLoS*
423 *one* 7(12):e53383.
- 424 22. Runft DL, *et al.* (2014) Zebrafish as a natural host model for *Vibrio cholerae* colonization and
425 transmission. *Applied and environmental microbiology* 80(5):1710-1717.
- 426 23. Hancock RE (2001) Cationic peptides: effectors in innate immunity and novel antimicrobials. *The*
427 *Lancet. Infectious diseases* 1(3):156-164.
- 428 24. Hancock RE & Sahl HG (2006) Antimicrobial and host-defense peptides as new anti-infective
429 therapeutic strategies. *Nature biotechnology* 24(12):1551-1557.
- 430 25. Mukherjee K, Rivera JJ, & Klibanov AM (2008) Practical aspects of hydrophobic polycationic
431 bactericidal "paints". *Applied biochemistry and biotechnology* 151(1):61-70.
- 432 26. Li P, *et al.* (2011) A polycationic antimicrobial and biocompatible hydrogel with microbe
433 membrane suctioning ability. *Nature materials* 10(2):149-156.
- 434 27. Atar-Froyman L, *et al.* (2015) Anti-biofilm properties of wound dressing incorporating nonrelease
435 polycationic antimicrobials. *Biomaterials* 46:141-148.
- 436 28. Cegelski L, Marshall GR, Eldridge GR, & Hultgren SJ (2008) The biology and future prospects of
437 antivirulence therapies. *Nature reviews. Microbiology* 6(1):17-27.
- 438 29. Lu HD, *et al.* (2015) Modulating *Vibrio cholerae* quorum-sensing-controlled communication using
439 autoinducer-loaded nanoparticles. *Nano letters* 15(4):2235-2241.
- 440 30. Ng WL, Perez L, Cong J, Semmelhack MF, & Bassler BL (2012) Broad spectrum pro-quorum-
441 sensing molecules as inhibitors of virulence in vibrios. *PLoS pathogens* 8(6):e1002767.
- 442 31. Klemm P, Vejborg RM, & Hancock V (2010) Prevention of bacterial adhesion. *Appl. Microbiol.*
443 *Biotechnol.* 88(2):451-459.
- 444 32. Krachler AM & Orth K (2013) Targeting the bacteria-host interface: Strategies in anti-adhesion
445 therapy. *Virulence* 4(4):284-294.
- 446 33. Faruque SM, *et al.* (2006) Transmissibility of cholera: in vivo-formed biofilms and their
447 relationship to infectivity and persistence in the environment. *Proceedings of the National*
448 *Academy of Sciences of the United States of America* 103(16):6350-6355.
- 449 34. Nelson EJ, *et al.* (2007) Complexity of rice-water stool from patients with *Vibrio cholerae* plays a
450 role in the transmission of infectious diarrhea. *Proceedings of the National Academy of Sciences*
451 *of the United States of America* 104(48):19091-19096.
- 452 35. Srivastava D, Hsieh ML, Khataokar A, Neiditch MB, & Waters CM (2013) Cyclic di-GMP inhibits
453 *Vibrio cholerae* motility by repressing induction of transcription and inducing extracellular
454 polysaccharide production. *Molecular microbiology* 90(6):1262-1276.
- 455 36. Jones CJ, *et al.* (2015) C-di-GMP Regulates Motile to Sessile Transition by Modulating MshA Pili
456 Biogenesis and Near-Surface Motility Behavior in *Vibrio cholerae*. *PLoS pathogens*
457 11(10):e1005068.
- 458 37. Townsley L & Yildiz FH (2015) Temperature affects c-di-GMP signalling and biofilm formation in
459 *Vibrio cholerae*. *Environmental microbiology* 17(11):4290-4305.
- 460 38. Camara M, Hardman A, Williams P, & Milton D (2002) Quorum sensing in *Vibrio cholerae*. *Nature*
461 *genetics* 32(2):217-218.
- 462 39. Waters CM, Lu W, Rabinowitz JD, & Bassler BL (2008) Quorum sensing controls biofilm formation
463 in *Vibrio cholerae* through modulation of cyclic di-GMP levels and repression of *vpsT*. *Journal of*
464 *bacteriology* 190(7):2527-2536.
- 465 40. Ng AN, *et al.* (2005) Formation of the digestive system in zebrafish: III. Intestinal epithelium
466 morphogenesis. *Developmental biology* 286(1):114-135.
- 467 41. Goldberg JB & Ohman DE (1984) Cloning and expression in *Pseudomonas aeruginosa* of a gene
468 involved in the production of alginate. *Journal of bacteriology* 158(3):1115-1121.

- 469 42. Heidelberg JF, *et al.* (2000) DNA sequence of both chromosomes of the cholera pathogen *Vibrio*
470 *cholerae*. *Nature* 406(6795):477-483.
- 471 43. Lodge J, Williams R, Bell A, Chan B, & Busby S (1990) Comparison of promoter activities in
472 *Escherichia coli* and *Pseudomonas aeruginosa*: use of a new broad-host-range promoter-probe
473 plasmid. *FEMS microbiology letters* 55(1-2):221-225.
- 474 44. Figurski DH, Pohlman RF, Bechhofer DH, Prince AS, & Kelton CA (1982) Broad host range plasmid
475 RK2 encodes multiple *kil* genes potentially lethal to *Escherichia coli* host cells. *Proceedings of the*
476 *National Academy of Sciences of the United States of America* 79(6):1935-1939.
- 477 45. O'Toole GA (2011) Microtiter dish biofilm formation assay. *Journal of visualized experiments* :
478 *JoVE* (47).
- 479 46. Bell AI, Gaston KL, Cole JA, & Busby SJ (1989) Cloning of binding sequences for the *Escherichia*
480 *coli* transcription activators, FNR and CRP: location of bases involved in discrimination between
481 FNR and CRP. *Nucleic acids research* 17(10):3865-3874.
- 482 47. Westerfield M (2000) *The Zebrafish Book*. (University Press Oregon, Eugene, OR).
- 483 48. Ritchie JM, *et al.* (2012) Inflammation and disintegration of intestinal villi in an experimental
484 model for *Vibrio parahaemolyticus*-induced diarrhea. *PLoS pathogens* 8(3):e1002593.

485

486

487

488

Supporting Information for

489

Capture of *Vibrio cholerae* by charged polymers inhibits pathogenicity by

490

inducing a sessile lifestyle

491

492 Nicolas Perez-Soto^{1,2}, Lauren Moule^{1,2}, Daniel N. Crisan^{2,3}, Ignacio Insua^{2,3}, Leanne M. Taylor-

493 Smith^{1,2}, Kerstin Voelz^{1,2}, Francisco Fernandez-Trillo^{2,3,*}, Anne Marie Krachler^{1,2,*}

494

495

496 This file contains:

497 Supporting Figures S1-S5

498 Supporting Tables S1 and S2

499 Supporting Materials and Methods

500

501

502

503

504

505

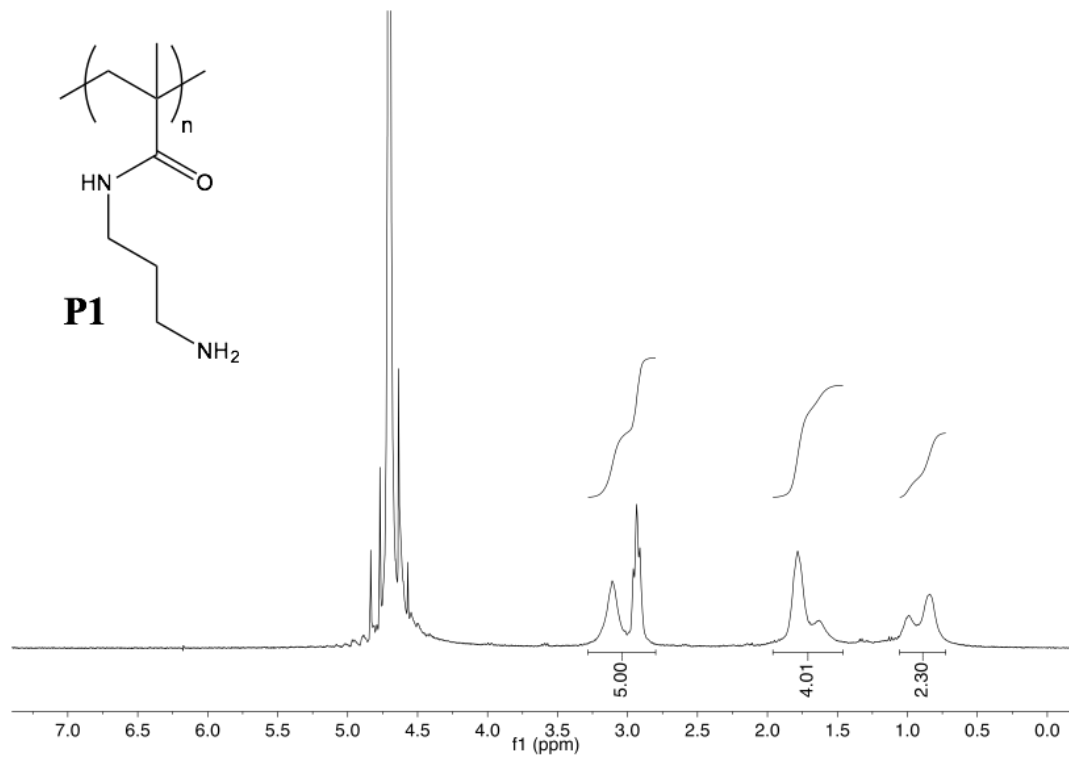
506

507

508

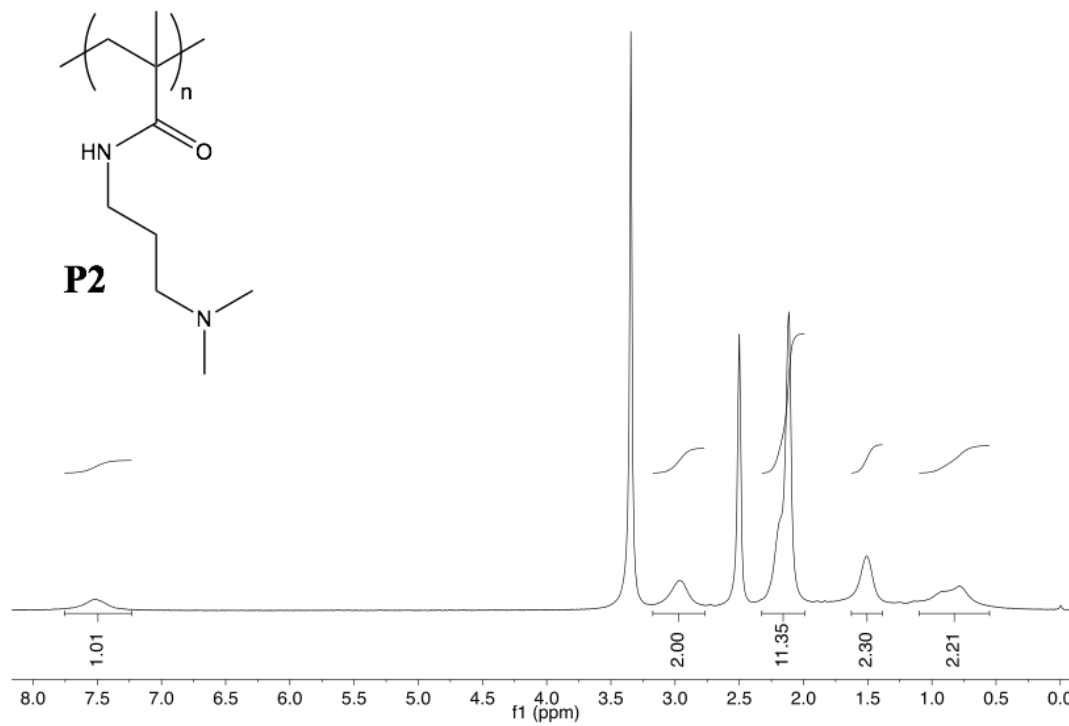
509

510 SUPPORTING FIGURES



511

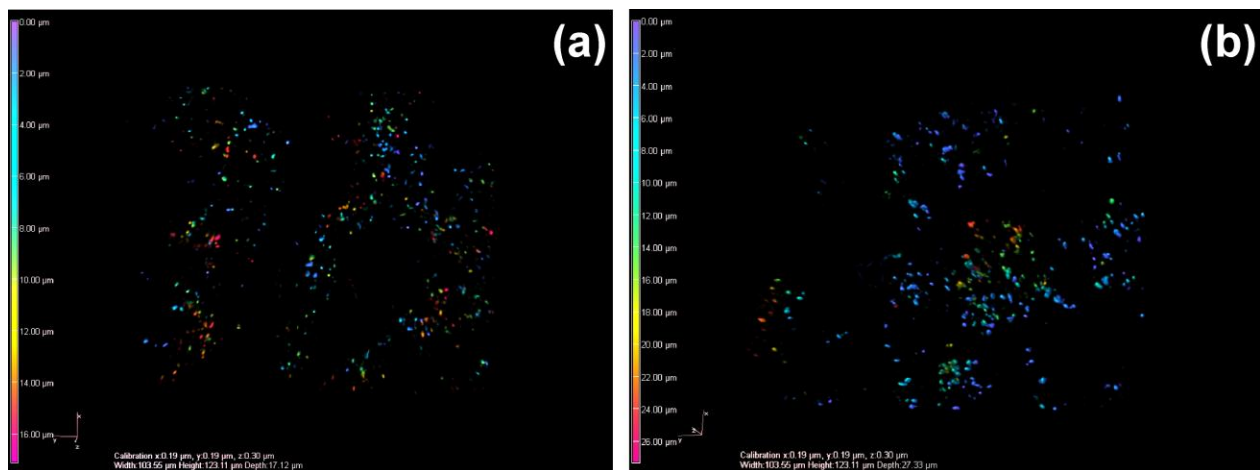
512 **Figure S11** ¹H-NMR (300 MHz, D₂O) spectrum of **P1**.



513

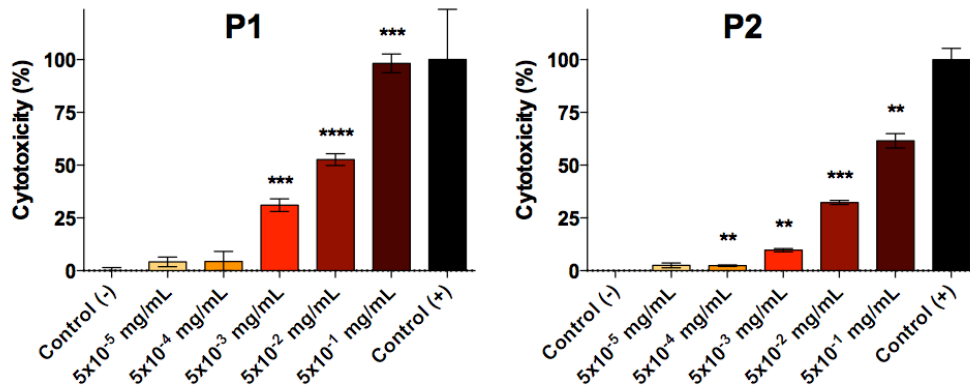
514 **Figure S2|** ¹H-NMR (300 MHz, DMSO-d₆) spectrum of **P2**.

515



516

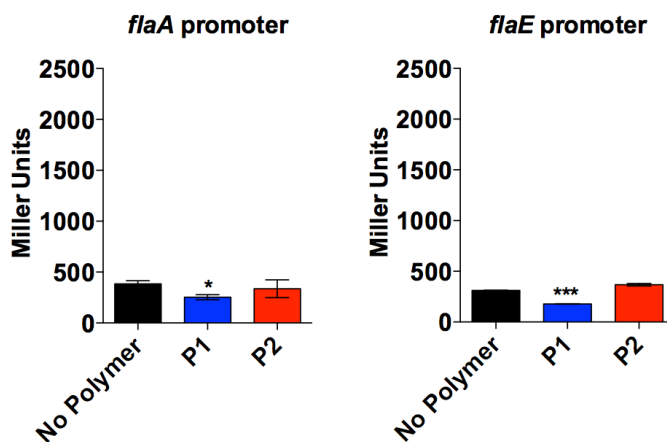
517 **Figure S3| Polymers induce rapid formation of three-dimensional bacterial clusters.** GFP-*V. cholerae* were
518 incubated with 0.5 mg/mL of P1 (a) or P2 (b) for 15 minutes, and z-stack images were collected using a spinning
519 disc confocal microscope. Maximum intensity projections are shown, with color-coded Z-depth. Total depth of the
520 clusters shown here are 17 and 27 μm, respectively.



521

522 **Figure S4| Effect of polymers on membrane integrity of cultured epithelial cells.** Solutions of polymers in
 523 DMEM at concentrations as indicated, were incubated with cultured Caco-2 intestinal epithelial cells for 7 hrs.
 524 Cytotoxic effect on host cells was quantified by measuring the amount of lactate dehydrogenase (LDH) released into
 525 the culture medium. Results were normalized to untreated Caco-2 cells (0%) and cells lysed with Triton X-100
 526 (100%). Results are means \pm s.e.m. of three independent experiments. Analysis of variance (ANOVA), followed by
 527 Tukey's post hoc test, was used to test for significance. Statistical significance was defined as $p < 0.01$ (**), $p < 0.001$
 528 (***), or $p < 0.0001$ (****).

529



530

531 **Figure S5| Effect of bacterial clustering on transcriptional regulation of flagella-driven motility.** Promoter
 532 activities of *flaA-lacZ* and *flaE-lacZ* fusions in *V. cholerae* were measured following 7 hours of growth in the
 533 absence (black) or in the absence (black) or presence of 0.05 mg/mL P1 (blue) or 0.5 mg/mL P2 (red) in DMEM at
 534 37 °C. Statistical significance was defined as $p < 0.05$ (*), or $p < 0.001$ (***).

535

536 **SUPPORTING TABLES**

537 **Table S1 | *V. cholerae* strains used in this study.**

Strain	Description	Source or reference
N16961	Wild-type; O1 biovar El Tor.	Heidelberg et al.(42)
NP5001	N16961 carrying promoterless pRW50-oriT plasmid; Tet ^R .	This study
NP5002	N16961 carrying pRW50-oriT plasmid containing the upstream region of <i>toxT</i> promoter; Tet ^R .	This study
NP5003	N16961 carrying pRW50-oriT plasmid containing the upstream region of <i>ctxAB</i> promoter; Tet ^R .	This study
NP5004	N16961 carrying pRW50-oriT plasmid containing the upstream region of <i>tcpA</i> promoter; Tet ^R .	This study
NP5005	N16961 carrying pRW50-oriT plasmid containing the upstream region of <i>aphA</i> promoter; Tet ^R .	This study
NPMW1	N16961 carrying pMW- <i>gfp</i> plasmid; Spect ^R .	Ritchie et al.(48)

538

539 **Table S2** Primers used in this study, with restriction sites underlined.

Primer	Sequence (5'-3')
pRW50 F	GTTCTCGCAAGGACGAGAATTTC
pRW50 R	AATCTTCACGCTTGAGATAC
aphApF1	TGCAGAATTCCTGGTTAACAAATCGCTAAATGTCAG
aphApR1	ATTCAAGCTTGTGTGGTAATGACATGTCTTCAATC
toxTpF1	TGTAGAATTCGATAAGATAACAGCCATATTCGTGG
toxTpR1	GATCAAGCTTTCCCAATCATTGCGTTCTACTC
ctxABpF1	GCTTGAATTCCTGTGGGTAGAAGTGAAACGG
ctxABpR1	TCATAAGCTTTATCTTTACCATATAATGCTCCCTTTG
tcpApF1	CTTAGAATTCGGTCTTATCATGAGCCGCC
tcpApR1	TGATAAGCTTTGCATATTTATATAACTCCACCATTTGTG

540

541 SUPPORTING MATERIALS AND METHODS

542 Polymer synthesis and characterization.

543 **Materials:** *N*-(3-aminopropyl)methacrylamide hydrochloride (APMAm), *N*-[3-
544 (dimethylamino)propyl]methacrylamide (DMAPMAm), 2,2'-azobis(2-methylpropionitrile)
545 (AIBN) and Dulbecco's Modified Eagle's Medium (DMEM) were purchased from Sigma-
546 Aldrich. 4,4'-azobis(4-cyanovaleric acid) (ACVA) and 2-mercaptoethanol were bought from Alfa
547 Aesar. Polyethylene glycol standards were purchased from Agilent Technologies. All other
548 chemicals were purchased from Fisher Scientific and VWR and were used without further
549 purification. Polymers were synthesized by radical polymerisation as described below.

550 **Instrumentation:** Polymers were characterized by Nuclear Magnetic Resonance (NMR) and Gel
551 Permeation Chromatography (GPC). NMR spectra were recorded on a Bruker Avance III
552 spectrometer operating at 300 MHz and fitted with a 5 mm BBFO probe. Chemical shifts (Figure
553 S1 and Figure S2) are reported in ppm (δ) referenced to the corresponding solvent signals:
554 DMSO-*d*6 ($\delta = 2.50$) and D₂O ($\delta = 4.79$). GPC was recorded on a Shimadzu Prominence LC-
555 20A, fitted with Shodex Asaphipak GF-510 HQ (300 × 7.5 mm, 5 μ m) and GF-310 HQ (300 ×
556 7.5 mm, 5 μ m) columns in series, and equipped with a Thermo Fisher Refractomax 521 detector.
557 GPC analysis was carried out using 100 mM acetate buffer at pH 2.9 as eluent at 40 °C and a
558 flow rate of 0.6 mL·min⁻¹. Molecular weights were calculated based on a standard calibration
559 method using polyethylene glycol.

560 **Synthesis and characterization of *p*(APMAm) (PI):** *N*-(3-aminopropyl)methacrylamide
561 (APMAm) hydrochloride (505.0 mg, 2.770 mmol), 4,4'-azobis(4-cyanovaleric acid) (ACVA)
562 (12.4 mg, 0.033 mmol) and 2-mercaptoethanol (1.0 μ L, 0.014 mmol) were dissolved in MilliQ
563 water (2.2 mL). This solution was degassed under argon for 10 minutes and then heated at 70 °C
564 under stirring for 17 hours. After this time, the reaction flask was opened to the air and the crude
565 was precipitated three times into diethyl ether (50 mL). The precipitate was freeze-dried and a
566 crystalline white solid was obtained (70.0 mg, 14% yield). ¹H-NMR (300 MHz, D₂O) δ (ppm):
567 3.11 (br, 3H, CH₃ backbone), 2.93 (br t, $J = 7.0$ Hz, 2H, CO-NH-CH₂), 1.78 (br, 2H, -CH₂-NH₂),
568 1.63 (br, 2H, -CH₂-CH₂-NH₂), 0.98 (br, 1H, CH₂ backbone), 0.83 (br, 1H, CH₂ backbone). Mn (GPC)
569 46997, D_M (GPC) 1.16.

570 **Synthesis and characterization of p(DMAPMAm) (P2):** *N*-[3-
571 (dimethylamino)propyl]methacrylamide (DMAPMAm) (2.2 mL, 12.025 mmol), 2,2'-azobis(2-
572 methylpropionitrile) (AIBN) (19.6 mg, 0.117 mmol) and 2-mercaptoethanol (4.0 μ L, 0.056
573 mmol) were dissolved in toluene (9.5 mL). This solution was degassed under argon for 10
574 minutes and then heated at 70 °C under stirring for 18 hours. After this time, the reaction flask
575 was opened to the air and the crude was precipitated twice: first into diethyl ether (200 mL) and
576 then into a diethyl ether/ hexane mixture (1:1) (100 mL). The precipitate was freeze-dried and a
577 crystalline white solid was obtained (1.66 g, 87% yield). ¹H-NMR (300 MHz, DMSO-*d*₆) δ
578 (ppm): 7.51 (br, 1H, CO-NH), 2.96 (br, 2H, CO-NH-CH₂), 2.19 (br, 5H, CH₂-N-(CH₃)₂ + CH₃
579 backbone), 2.11 (br, 6H, N-(CH₃)₂), 1.50 (br, 2H, CH₂-CH₂-N), 0.78 (br, 2H, CH₂ backbone). Mn
580 (buffer GPC) 46331, *D*_M (buffer GPC) 1.14.

581 **Bacterial strains and culture conditions.** *Vibrio cholerae* strains used in this study (Table S1)
582 were derived from the El Tor strain N16961 used as parental strain. Strains were propagated at 37
583 °C in Luria-Bertani (LB) broth supplemented with 50 μ g/ μ L spectinomycin, 30 μ g/ μ L kanamycin
584 or 10 μ g/ μ L tetracycline where selection was required. Plasmids were introduced into *V. cholerae*
585 by conjugation, as previously described (41). Briefly, aliquots of overnight cultures of *V.*
586 *cholerae* N16961, *E. coli* DH5a carrying the desired plasmid (donor) and an *E. coli* SM10 helper
587 strain carrying pRK2013 were mixed at a volumetric ratio of 1:2:2 and spotted onto brain-heart
588 infusion (BHI) agar. Following overnight incubation, spots of bacterial growth were dislodged
589 and suspended in 3 mL of PBS. 100 μ L of bacterial suspension were plated onto M9 media
590 containing 50 μ g/ μ L of spectinomycin. Resulting colonies were checked by PCR and sequencing
591 in the case of pRW50-oriT constructs, and also by screening for green fluorescence in the case of
592 pMW-*gfp* transformants.

593 **Plasmid construction.** Primers used for cloning and sequencing the constructs used in this study
594 are listed in **Table S2** and were designed based on the sequence of *V. cholerae* N16961 (42).
595 Primers were paired as appropriate to amplify upstream regions of *toxT*, *ctxAB*, *tcpA*, *aphA*, *flaA*
596 and *flaE* (**Figure 4** and **Figure S5**). Amplified DNA was digested using EcoR1 and HindIII, and
597 ligated into digested pRW50-oriT vector (gift from the Grainger lab). The vector is a derivative
598 of pRW50 (43), which has been modified by inserting the *oriT* sequence from the vector pRK2

599 (44). The resulting reporter constructs were used to transform *V. cholerae* and the resulting
600 strains are listed in **Table S1**.

601 **Imaging and sizing of bacterial clusters.** An overnight culture of *V. cholerae* was diluted to an
602 OD₆₀₀ of 1.0 in DMEM without phenol red and polymers were added to final concentrations
603 ranging from 0-0.5 mg/mL (**Figure 1** and **Figure S3**). For imaging of clusters, aliquots were
604 taken after 15 and 60 min of incubation and mounted with ProLong® Antifade Gold solution
605 (LifeTechnologies). Cured samples were visualized using a Nikon-Eclipse TE2000-U microscope
606 and Plan Apo 60x/ 1.40 NA oil DIC objective (Nikon) and captured with QICAM Fast1394
607 camera (Q imaging). Representative images were taken using Nikon NIS-Elements software and
608 prepared with ImageJ and Corel Draw X5 software. The size distribution of bacterial clusters was
609 determined using a Mastersizer 3000 (Malvern) through a period of time of 10 minutes following
610 addition of polymer. P1 was added at 5×10^{-2} mg/mL and 5×10^{-1} mg/mL with stirring and
611 recorded particle diffraction was plotted as percentage of the particles with a diameter larger than
612 2 μ m. The cutoff size for clusters versus individual bacteria was determined on the median
613 diameter of particles from a sample containing no polymer (2 μ m).

614 **Determination of bacterial growth and membrane integrity.** Overnight cultures of GFP-
615 expressing *V. cholerae* were diluted into DMEM containing 50 μ g/ μ L of spectinomycin to an
616 OD₆₀₀ of 0.02 as starting density. Polymers aliquots were added to give the desired final
617 concentrations (**Figure 2**) in 200 μ L culture using a 96-well plate. The plate was covered with a
618 BEM-1 breathe easy gas permeable membrane to avoid evaporation and incubated at 37 °C with
619 constant shaking at 200 rpm. GFP fluorescence was recorded every 30 minutes over 24 hours
620 using a FLUOstar Omega plate reader. Membrane integrity of *V. cholerae* cells was assessed by
621 fluorescent-activated cell sorting (FACS) using the LIVE/DEAD BacLight™ kit
622 (LifeTechnologies). Overnight cultures were diluted to an OD₆₀₀ of 1.0 in 1 mL of DMEM
623 without phenol red, and containing polymers at final concentrations ranging from 0 to 0.5 mg/mL
624 and incubated for 20 hours (**Figure 2**). Following incubation, samples were stained according to
625 the manufacturer's instructions. Readings were taken on an Attune Flow Cytometer, at a flow of
626 100 μ L/min counting up to 10,000 events. Samples containing no polymer were used as "LIVE"
627 controls. In the case of "DEAD" controls, DMEM was replaced by 70% 2-propanol and

628 incubated for 1 h. Prior to staining, 2-propanol was removed and cells were washed once and
629 resuspended in fresh DMEM to carry out the staining procedure.

630 **Quantification of biofilm formation (Figure 3a).** The amount of biofilm was determined by
631 crystal violet staining, as previously described (45). Briefly, *V. cholerae* was exposed to different
632 concentrations of polymers and incubated overnight at 37°C with shaking in a 96-well plate.
633 Cultures were removed and biofilm was rinsed with PBS and stained with 200 µL of 1% crystal
634 violet solution in water. After 30 minutes, the crystal violet solution was removed and the well
635 was rinsed again with PBS. In order to detach the dye, 200 µL of 95% ethanol was added to each
636 well. The amount of biofilm was determined by measuring at a wavelength 595 nm.

637 **Imaging of biofilm formation (Figure 3b-d).** Biofilms of GFP-*V. cholerae* were grown for 20
638 hours at 37°C in 96-well glass-bottom plates containing bacteria at an initial OD₆₀₀ of 0.2 in
639 DMEM only, or DMEM containing 0.05 mg/mL P1, or 0.05 mg/mL P2. Following incubation,
640 plates were rinsed with PBS, samples fixed with 4% formaldehyde in PBS for 15 minutes and
641 then washed with PBS. DNA was stained with 10 µg/mL Hoechst in PBS for 10 minutes.
642 Samples were imaged using a Zeiss Axio Observer.Z1 microscope, Zeiss 40x/1.4 Plan
643 Apochromat, objective, ORCA-Flash4.0 camera (Hamamatsu) and ZEN 2.0.0.10 software,
644 Images were processed using Image J and Corel Draw X5.

645 **Transcriptional assays: β-galactosidase activity.** *V. cholerae* reporter strains were assayed for β-
646 galactosidase activity as previously described (46). Briefly, *V. cholerae* cultures were diluted to
647 an OD₆₀₀ of 0.2 and incubated for 7 hours at 37 °C in DMEM containing polymers. Separate
648 aliquots were taken and used to measure β-galactosidase activity, or washed with PBS and
649 resuspended in high salt solution to disrupt clusters prior to measuring OD₆₀₀. Transcriptional
650 activity (in Miller Units) was calculated as previously described (46).

651 **Cytotoxicity in Caco-2 cells.** Overnight cultures of the GFP-expressing *V. cholerae* were grown
652 in LB at 37 °C. Prior to infection, cultures were adjusted to an MOI of 10 and incubated for 1
653 hour in 1 mL of DMEM without phenol red and polymers as indicated, at 30 °C. Caco-2 cells
654 were washed with PBS to remove media containing antibiotics and infections were started by
655 transferring the solution of bacteria into the wells. Plates were centrifuged at 1000x g for 5 min at
656 20 °C to synchronize the infections. After an incubation of 7 hours at 37 °C under 5% CO₂,

657 supernatants were used to measure lactate dehydrogenase (LDH) activity using LDH Cytotoxicity
658 Detection Kit (Takara Cloneteck) according to the manufacturer's instructions. The data was
659 expressed as percentage of cytotoxicity, normalized to untreated cells (0%) and 0.1% Triton X-
660 100 lysed cells (100% lysis) and was calculated according to the formula: % cytotoxicity=100 x
661 $[(\text{OD}_{490} \text{ for experimental release} - \text{OD}_{490} \text{ for spontaneous release}) / (\text{OD}_{490} \text{ for maximum}$
662 $\text{release} - \text{OD}_{490} \text{ for spontaneous release})]$.

663 **Zebrafish care and maintenance.** Zebrafish (*Danio rerio* wild type strain AB) were kept in a
664 recirculating tank system at the University of Birmingham Aquatic Facility. Zebrafish were kept
665 under a 14h-10h light-dark cycle with water temperature maintained at 28 °C. Zebrafish care,
666 breeding and experiments were performed in accordance with the Animal Scientific Procedures
667 Act 1986, under Home Office Project License 40/3681. After collection of eggs, larvae were kept
668 in a diurnal incubator under a 14h-10h light-dark cycle with the temperature maintained at 33 °C.
669 Eggs were maintained at 40 eggs per 50 ml in E3 media plus 0.00003% methylene blue for 8 h
670 and E3 media plus 26.6 µg/ml 1-phenyl-2-thiourea (PTU) to inhibit melanization. The fish line
671 used was wild-type AB zebrafish. All zebrafish care and husbandry procedures were performed
672 as described previously (47).

673 **Infection of zebrafish embryos with *V. cholerae*.** Prior to infection, 10^6 and 10^7 CFU/mL of *V.*
674 *cholerae* were incubated in 3 mL of E3 medium containing polymers as indicated in the figure
675 legends. After 1 hour of incubation to ensure cluster formation, zebrafish embryos (5 d.p.f) were
676 placed into cluster solutions and incubated with rotation at 25 °C for 6 hours. Embryos were
677 euthanised with an overdose of Tricaine-S (1600 µg/mL) and homogenised by washing the
678 embryos with PBS and incubating them in 1% Triton X-100 for 30 minutes. Lysates were passed
679 several times through a needle to homogenize and 100 µL of the resulting solution, as well as
680 serial dilutions, were plated onto TCBS agar and colonies counted following overnight
681 incubation at 37 °C.

682 **Imaging of infected Caco-2 cells and zebrafish embryos.** In the case of samples for imaging,
683 Caco-2 cells were seeded onto sterilized glass cover slips inserted into wells of the plate. Imaging
684 of infected Caco-2 cells was done by fixing the samples with 4% formaldehyde in PBS for 15
685 minutes and then washing with PBS. Cells were permeabilized by adding 0.1% Triton X-100 in
686 PBS and incubation at room temperature for 5 minutes, and washed three times with PBS.

687 Samples were stained with 10 $\mu\text{g}/\text{mL}$ Hoechst and 66 ng/mL of rhodamine-phalloidin in the dark
688 for 10 minutes to visualize DNA and F-actin, respectively. Staining was followed by three
689 washing steps with PBS (5 minutes each). Samples were mounted using antifade gold mounting
690 solution (Life-Technologies) and cured overnight at 22 $^{\circ}\text{C}$ prior to visualization. Visualization of
691 zebrafish embryos was done by directly mounting the embryos in 0.4% low melting point
692 agarose containing 160 $\mu\text{g}/\text{mL}$ of Tricaine-S. Samples were viewed under a Zeiss Axio
693 Observer.Z1 microscope with 63x/1.4 Plan Achromat objective for the Caco-2 infection and
694 20x/0.8 Plan Achromat objective in the case of the larvae. Images were processed using
695 ImageJ software.

696

697

698